Archival Report

Biological Psychiatry: CNNI

Basal Ganglia Pathways Associated With Therapeutic Pallidal Deep Brain Stimulation for Tourette Syndrome

Kara A. Johnson, Gordon Duffley, Thomas Foltynie, Marwan Hariz, Ludvic Zrinzo, Eileen M. Joyce, Harith Akram, Domenico Servello, Tommaso F. Galbiati, Alberto Bona, Mauro Porta, Fan-Gang Meng, Albert F.G. Leentjens, Aysegul Gunduz, Wei Hu, Kelly D. Foote, Michael S. Okun, and Christopher R. Butson

ABSTRACT

BACKGROUND: Deep brain stimulation (DBS) targeting the globus pallidus internus (GPi) can improve tics and comorbid obsessive-compulsive behavior (OCB) in patients with treatment-refractory Tourette syndrome (TS). However, some patients' symptoms remain unresponsive, the stimulation applied across patients is variable, and the mechanisms underlying improvement are unclear. Identifying the fiber pathways surrounding the GPi that are associated with improvement could provide mechanistic insight and refine targeting strategies to improve outcomes.

METHODS: Retrospective data were collected for 35 patients who underwent bilateral GPi DBS for TS. Computational models of fiber tract activation were constructed using patient-specific lead locations and stimulation settings to evaluate the effects of DBS on basal ganglia pathways and the internal capsule. We first evaluated the relationship between activation of individual pathways and symptom improvement. Next, linear mixed-effects models with combinations of pathways and clinical variables were compared in order to identify the best-fit predictive models of tic and OCB improvement.

RESULTS: The best-fit model of tic improvement included baseline severity and the associative pallido-subthalamic pathway. The best-fit model of OCB improvement included baseline severity and the sensorimotor pallido-subthalamic pathway, with substantial evidence also supporting the involvement of the prefrontal, motor, and premotor internal capsule pathways. The best-fit models of tic and OCB improvement predicted outcomes across the cohort and in cross-validation.

CONCLUSIONS: Differences in fiber pathway activation likely contribute to variable outcomes of DBS for TS. Computational models of pathway activation could be used to develop novel approaches for preoperative targeting and selecting stimulation parameters to improve patient outcomes.

https://doi.org/10.1016/j.bpsc.2020.11.005

Tourette syndrome (TS) is a complex neuropsychiatric disorder characterized by repetitive involuntary movements or vocalizations referred to as tics. TS is also frequently associated with comorbidities, such as obsessive-compulsive behavior (OCB) and other behavioral and psychiatric disorders (1–3). Deep brain stimulation (DBS) therapy can effectively reduce tic severity, improve comorbidities such as OCB, and improve the quality of life for select patients with severe, treatment-refractory TS (4). Several open-label and retrospective studies have reported significant symptom improvements with DBS (5–8), and randomized controlled trials have shown mainly positive results with some conflicting evidence (9–12). Although many patients with TS have experienced substantial improvements with DBS, outcomes remain variable across patients, with only 54% of patients experiencing at least a 50% improvement in tics (13). It is critical to determine how to apply DBS in order to consistently improve tics and comorbidities in individual patients.

The underlying pathophysiology of TS and comorbid OCB is not fully understood; however, both are thought to involve the cortico-basal ganglia-thalamo-cortical (CBGTC) networks, which comprise partially segregated loops involved in sensorimotor, limbic, and associative processing (14,15). Based on the involvement of the CBGTC circuitry in TS, the most common DBS targets are the globus pallidus internus (GPi) (anteromedial and posteroventral subregions) and regions of the centromedial thalamus (13). The anteromedial GPi may be a particularly effective target for patients with TS and prominent comorbid OCB (16,17), or potentially patients with treatment-refractory obsessive-compulsive disorder (OCD) without TS (18). Recent studies have investigated the neurophysiological activity in the GPi associated with tics (19–21) and the potential

ISSN: 2451-9022

mechanisms of GPi DBS for TS (22,23). However, the reported mechanisms have yet to be directly linked to symptom improvement, and it remains unclear how to optimally modulate the CBGTC circuitry with GPi DBS to improve symptoms effectively.

The stimulation applied during GPi DBS is variable across patients owing to differences in lead location and stimulation parameters, and stimulation often extends outside the target (24,25). Variability in stimulation with GPi DBS also applies to nearby fiber pathways with varying activation levels across patients, stimulation settings, and even hemispheres. Our previous work revealed that stimulation location alone was not predictive of tic or OCB improvement (24). However, our recent study found that structural connectivity of the site of stimulation to distributed cortical and subcortical networks predicted tic improvement following GPi DBS (26). This work provided preliminary evidence that differences in stimulation were linked to clinical outcomes, but it is unknown which local fiber pathways should be modulated to improve tics or comorbid OCB. The need to identify effective neuroanatomical structures for stimulation is especially critical in TS because the time course for patients' symptoms to respond to DBS can be on the order of months (24,27), and the acute effects of stimulation on tics or OCB are often not immediately observed during programming sessions.

The objective of this study was to identify the fiber pathways surrounding the GPi, including the basal ganglia and internal capsule pathways, that when stimulated were associated with improvement in tics and comorbid OCB in a multicenter cohort of patients who underwent bilateral GPi DBS for TS. Multiple outcome measures and stimulation settings per patient were used to evaluate the effects of stimulation over time with computational models of fiber activation. We first analyzed the relationship between activation of individual pathways and symptom improvement, and then we expanded to evaluate combinations of fiber pathways and clinical variables to identify predictive models of tic and comorbid OCB improvement. The present study aimed to provide preliminary evidence of the pathways involved in the underlying mechanisms of symptom improvement and develop novel predictive models that could guide the application of GPi DBS therapy for treatment-refractory TS to consistently improve symptoms.

METHODS AND MATERIALS

Cohort Data

Retrospective longitudinal data of patients who underwent bilateral DBS for TS targeted to the GPi were collected from the International TS DBS Registry and Database (28) (https://tourettedeepbrainstimulationregistry.ese.ufhealth.org) in collaboration with the International Neuromodulation Registry (https://neuromodulationregistry.org). The dataset included demographics, preoperative structural T1-weighted magnetic resonance imaging (MRI), postoperative MRI or computed tomography, baseline and follow-up clinical rating scale scores, and stimulation settings. The inclusion criteria were high-quality pre- and postoperative imaging [described previously (24)], baseline clinical rating scale scores, and at least one follow-up time point with clinical rating scale scores and stimulation settings. The Yale Global Tic Severity Scale (YGTSS) total score (29) was used to assess TS severity and impairment, and the Yale-Brown Obsessive-Compulsive Behavior Scale (Y-BOCS) total score (30) was used to assess the severity of comorbid OCB.

Preprocessing of Patient Imaging

The imaging of each patient was processed to carefully localize the neuroanatomical position of each DBS lead and register all patients' preoperative imaging to a common atlas space. Detailed methods have been previously described (24). Briefly, for each patient, the postoperative imaging was used to manually localize the DBS leads using SCIRun 4 software (http://www.sci.utah.edu/cibc-software/scirun.html) and was rigidly registered to the preoperative MRI. The Advanced Normalization Tools (http://stnava.github.io/ANTs/) SyN algorithm (31) was used to nonlinearly register the preoperative MRI to a cohort atlas comprising imaging from TS DBS patients in the full dataset (24) that was also aligned to Montreal Neurological Institute space using the ICBM 2009b Nonlinear Asymmetric atlas (32,33). This series of image registrations yielded a set of transformations between Montreal Neurological Institute space and native preoperative space for each patient to compare the computational models of fiber tract activation across the cohort.

Computational Models of Fiber Tract Activation

Computational models were constructed to estimate the effects of DBS on the fiber pathways surrounding the GPi in order to identify the fiber tracts that were commonly activated during GPi DBS and identify those associated with symptom improvement. We modeled fiber pathways surrounding the GPi that were previously defined by expert anatomists (34), including basal ganglia pathways and subdivisions of the internal capsule (shown in Figure 1). We also modeled fiber pathways that were positively or negatively associated with OCD improvement in a recent study by Li *et al.* (35) to determine whether activation of these pathways was also associated with improvement in OCB in our TS cohort. To model the neurophysiological effects of stimulation on the pathways, we computed the voltage solution of each stimulation setting, constructed axon models along the trajectory of each individual tract, and then simulated the axonal response to the stimulation. Details about the modeled fiber pathways and the computational modeling methods are provided in the Supplement.

Quantification of Fiber Pathway Activation

Using the results of the fiber tract activation computational models, maps were generated to identify the fiber tracts within the pathways that were frequently activated during GPi DBS. We visualized the percentage of the total number of stimulation settings across all patients that activated each individual fiber tract in each pathway. Next, we characterized activation at the pathway level within each hemisphere. For each stimulation setting, the percent activation of each pathway was calculated for the left and right hemispheres separately (% activation =

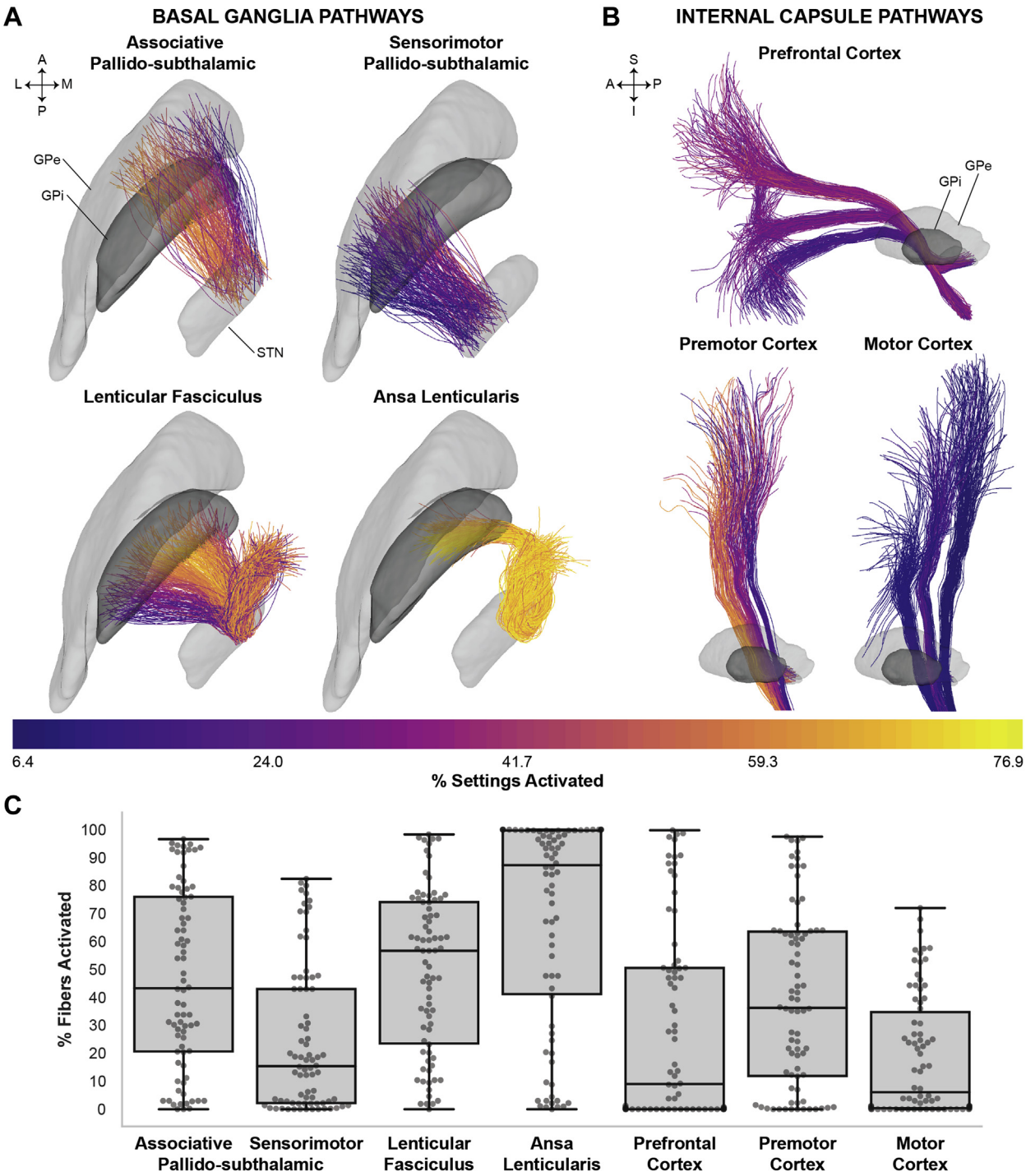

Figure 1. Fiber tract activation of the **(A)** basal ganglia pathways and **(B)** internal capsule pathways across all patients and stimulation settings. The colormap in panels **(A)** and **(B)** denotes the percentage of settings that activated each fiber tract across bilateral settings (n = 156) over all follow-up time points for the patients in the cohort (n = 35). **(C)** Boxplots and individual data points of the bilateral percent activation of the pathways across all patients and stimulation settings. A, anterior; GPe, globus pallidus externus; GPi, globus pallidus internus; I, inferior; L, lateral; M, medial; P, posterior; S, superior; STN, subthalamic nucleus.

number of active fibers/total number of fibers in pathway), and interhemispheric symmetry was calculated (see Supplement). For all remaining statistical models, we combined the two hemispheres by computing the bilateral percent activation of each pathway (the average of % left and % right) for each stimulation setting. To determine which pathways were commonly coactivated, pairwise Pearson correlations were performed of the bilateral percent activation for all pathways (Table S1).

Statistical Analysis

Statistical Models of Pathway Activation and Clinical Outcomes. We first evaluated the relationship between activation of individual pathways and symptom improvement. Pearson correlations of the bilateral percent activation of each pathway and the raw improvement in the clinical rating scale scores (raw improvement = baseline score – follow-up score) were computed. A positive raw improvement score represented a reduction in symptom severity compared with baseline. The Benjamini-Hochberg false discovery rate (FDR) method was applied to correct for multiple comparisons (36). For all statistical analyses, a threshold of $p < .05$ was used to define statistical significance.

The Pearson correlations provide information about the general relationship between activation of each individual pathway and symptom improvement. However, therapeutic effects of GPi DBS may be related to activation of combinations of fiber pathways and other clinical variables. We therefore compared models of different combinations of fiber pathways and clinical variables to identify the model that best predicted symptom improvement while accounting for repeated measures within patients. Linear mixed-effects models were generated with the raw improvement in the clinical rating scale score as the dependent variable. The models included patient-specific random intercepts, and the independent variables (fixed effects) included bilateral percent activation of each pathway, time point (in months since surgery), and baseline clinical rating scale score. We identified the best-fit model(s) for each clinical outcome measure by minimizing the Akaike information criterion (AIC) (37) [corrected for small sample sizes (38,39)] across the possible models with combinations of fiber pathways and clinical variables. Details about the AIC method for model selection are provided in the Supplement.

Prediction of Clinical Outcomes. We evaluated the predictive power of the best-fit model for each clinical outcome. Raw improvement scores were predicted using the fixed effects of the model in the whole cohort, and k-fold cross-validation (k = 10) was used to verify that the model was able to predict out-of-sample data and was not overfit to the present dataset. The predictive power of the models was evaluated by performing a Pearson correlation (r_p) as well as by performing a repeated-measures correlation (r_{rm}) (40) to compare the clinical scores and the predicted scores while accounting for repeated outcome measures for each patient. The prediction error in k-fold cross-validation was calculated for each data point (error = predicted score – clinical score), and a single prediction error was obtained for each patient by averaging across time points.

RESULTS

Cohort Characteristics

The cohort included 35 patients who underwent bilateral GPi DBS for treatment-refractory TS, and the demographic and clinical characteristics are described in Table 1. The longitudinal dataset included a total of 90 follow-up data points combined across patients and over time with recorded YGTSS scores and stimulation settings. Of the 90 follow-up data points, there were 78 bilateral settings (n = 156 combined across hemispheres), and 12 patients had clinical outcome scores recorded at 1 month postsurgery before stimulation was turned on as an additional control to account for any microlesion effects (9). The present cohort is a subset of a larger cohort reported in our previous studies (24,26), which included detailed statistical analyses of the longitudinal clinical outcomes and visualization of the active contact locations.

Variability in Fiber Pathway Activation

The maps of fiber pathway activation across all patients and stimulation settings (Figure 1A, B) showed that a relatively higher proportion of stimulation settings activated the associative pallido-subthalamic pathway, the ansa lenticularis, the anterior lenticular fasciculus, and the prefrontal and premotor internal capsule pathways. The distributions of the bilateral percent activation of each pathway (Figure 1C) showed substantial variability in stimulation across the cohort. Select pathways showed notable asymmetric activation across hemispheres; however, relatively few patients were programmed with asymmetric stimulation settings (Figure S1). Pairwise correlations of the bilateral percent activation of the pathways showed common coactivation of the basal ganglia pathways and the internal capsule pathways (Table S1).

Fiber Pathways Associated With Tic Improvement

We first assessed the correlation between improvement in YGTSS scores and activation of the basal ganglia pathways and internal capsule pathways across all patients and stimulation settings (Table 2). The bilateral percent activation of the associative pallido-subthalamic pathway, the ansa lenticularis, and the internal capsule tracts projecting to the prefrontal cortex was significantly correlated with tic improvement ($p < .05$, FDR corrected); notably, these three pathways were surrounding the anterior pallidum.

Next, we identified the combinations of pathways and clinical variables that best predicted the raw YGTSS improvement scores (Table S2). The best-fit linear mixed-effects model with the minimum AIC (model 1) included baseline YGTSS score ($\beta = .62$, $p < .001$) and bilateral percent activation of the associative pallido-subthalamic pathway ($\beta = .39$, $p < .001$) (visualized in Figure 2A). There were no additional models within the threshold for having substantial empirical evidence compared with the best-fit model (38), including any models with combinations of fiber pathways that were significantly correlated with improvement (Table 2). For comparison, a model with only the clinical variables (baseline YGTSS score and time point since surgery) had an AIC over 26 points greater than model 1, indicating essentially no empirical support relative to the best-fit model.

Table 1. Cohort Demographics and Clinical Outcomes

Characteristic	Value
Total Number of Patients	35
Sex, Male/Female	26/9
Age at Surgery, Years	29.5 (9.6)
Latest Follow-up Time Point, Months	24 (30, 1–81)
Number of Follow-up Time Points per Patient	3 (7, 1–8)
YGTSS: Baseline (n = 35)	77.1 (20.1)
YGTSS: Raw Improvement (Latest Follow-up Time Point) (n = 35)	35.6 (23.4)
YGTSS: Baseline (n = 12 Patients With Off-Stimulation Data)	84.7 (12.8)
YGTSS: Raw Improvement (1 Month, Off Stimulation) (n = 12)	10.3 (16.5)
Y-BOCS: Baseline (n = 28)	22.2 (11.7)
Y-BOCS: Raw Improvement (Latest Follow-up Time Point) (n = 28)	7.5 (9.4)
Y-BOCS: Baseline (n = 11 Patients With Off-Stimulation Data)	15.0 (9.6)
Y-BOCS: Raw Improvement (1 Month, Off Stimulation) (n = 11)	2.1 (2.6)

Values are n, mean (SD), or median (interquartile range, range).
Y-BOCS, Yale-Brown Obsessive Compulsive Scale; YGTSS, Yale Global Tic Severity Scale.

The best-fit model with the minimum AIC (model 1 in Table S2) was used to predict raw YGTSS improvement scores at each follow-up time point for each patient (Figure 2). The clinical improvement scores and the predicted improvement scores were significantly correlated (r_{rm} = .69; 95% confidence interval [CI], .52–.81; $p < .001$; r_p = .42; 95% CI, .41–.43; $p < .001$) (Figure 2B). The model was also predictive in k-fold cross-validation (r_{rm} = .65; 95% CI, .47–.78; $p < .001$; r_p = .36; 95% CI, .35–.37; $p < .001$). The median error of the predicted scores compared with the clinical scores in k-fold cross-validation was 3.36 points (Figure 2C).

Fiber Pathways Associated With OCB Improvement

Across all patients and stimulation settings, improvement in the Y-BOCS total score was significantly correlated with the bilateral percent activation of the associative and sensorimotor pallido-subthalamic pathways and all three of the internal capsule pathways ($p < .01$, FDR corrected) (Table 3). Additionally, activation of the positively associated pathway from Li *et al.* (35) was significantly correlated with OCB improvement (r_p = .45; 95% CI, .45–.46; $p < .001$, FDR corrected). In contrast, neither the pallido-thalamic pathways (lenticular fasciculus and ansa lenticularis) nor the negatively-associated pathway from Li *et al.* (35) (r_p = .17; 95% CI, .16–.18; p = .201) were significantly correlated with improvement.

The linear mixed-effects models of improvement in the Y-BOCS score are reported in Table S3. The best-fit model with the minimum AIC included baseline Y-BOCS score (β = .42, $p < .001$) and bilateral percent activation of the sensorimotor pallido-subthalamic pathway (β = .13, p = .002). Three additional models met the criteria for having substantial empirical evidence of a similar level as the minimum AIC model, which comprised baseline Y-BOCS total score and portions of the internal capsule. Compared with the best-fit model, the models with combinations of pathways that were significantly correlated with improvement and the model with only clinical variables (Table 3) yielded AIC values outside the threshold for substantial evidence.

The best-fit model with the minimum AIC (model 1 in Table S3), comprising baseline Y-BOCS score and the bilateral percent activation of the sensorimotor pallido-subthalamic pathway, was used to predict raw Y-BOCS improvement scores for each follow-up time point for each patient (Figure 3). The predicted scores were significantly correlated with the clinical scores (r_p = .61; 95% CI, .60–.62; $p < .001$; r_{rm} = .41; 95% CI, .12–.64; p = .008) (Figure 3B). The model was also predictive under k-fold cross-validation (r_p = .54; 95% CI, .53–.55; $p < .001$; r_{rm} = .41; 95% CI, .12–.64; p = .008). The median error of the predicted scores compared with the clinical scores was −0.49 points (Figure 3C).

DISCUSSION

Patient responses to GPi DBS for TS remain variable, the applied stimulation varies substantially across patients and stimulation settings, and the fiber pathways that mediate symptom

Table 2. Correlations of Pathway Activation and Tic Improvement

Pathway	Correlation Coefficient (r_p)	95% CI	p Value
Associative Pallido-subthalamic	.28	.27–.29	.018[a]
Sensorimotor Pallido-subthalamic	.03	.02–.04	.792
Lenticular Fasciculus	.22	.21–.22	.069
Ansa Lenticularis	.30	.30–.31	.013[a]
IC: Prefrontal Cortex	.34	.33–.34	.008[a]
IC: Premotor Cortex	.17	.17–.18	.140
IC: Motor Cortex	.08	.07–.09	.531

CI, confidence interval; IC, internal capsule, r_p, Pearson correlation.
[a]$p < .05$, false discovery rate corrected.

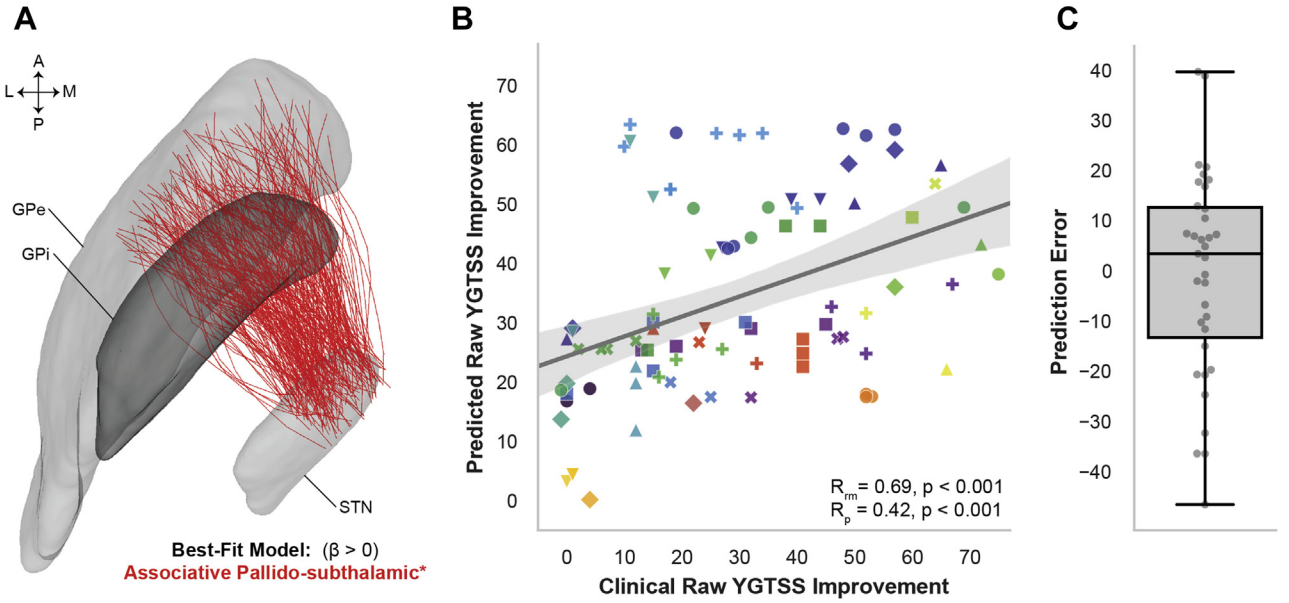

Figure 2. Tic improvement predicted using baseline severity and bilateral percent activation of the associative pallido-subthalamic pathway. **(A)** Visualization of the pathway included in the best-fit model of tic improvement (model 1 in Table S2). **(B)** The best-fit model was predictive of raw Yale Global Tic Severity Scale (YGTSS) improvement scores for patients in the cohort (n = 35) across time points (n = 90). Individual patients are denoted by unique color-marker pairs. **(C)** Boxplot and individual data points of the prediction error in k-fold cross-validation, in which error = clinical score – predicted score. A, anterior; GPe, globus pallidus externus; GPi, globus pallidus internus; L, lateral; M, medial; P, posterior; r_p, Pearson correlation; r_{rm}, repeated-measures correlation; STN, subthalamic nucleus.

improvement are unclear. The objective of this study was to identify the fiber pathways surrounding the GPi, including the basal ganglia pathways and the internal capsule, that were associated with improvement in tics and comorbid OCB. We report novel predictive approaches based on computational models of activation of major fiber pathways surrounding the GPi, which could be instrumental in guiding preoperative targeting or optimizing stimulation parameters for improving tics and OCB in future patients undergoing DBS therapy for TS.

Variability and Interhemispheric Symmetry in Pathway Activation

Computational models of stimulation showed that there was notable variability in pathway activation across all patients and stimulation settings (Figure 1). Stimulation frequently spread outside of the GPi, indicated by coactivation of the basal ganglia pathways and the internal capsule pathways (Table S1). Variability in pathway activation across patients is attributed to differences in lead location and trajectory relative to the fiber pathways combined with differences in stimulation settings. We observed similar variability in anatomical regions stimulated in a previous study (24), but by modeling the activation of individual fiber tracts, we were able to account for differences in fiber orientation relative to the electrodes (41).

The present study quantified interhemispheric symmetry of stimulation (Figure S1), a concept that is seldom explored in studies of bilateral DBS. Interhemispheric asymmetry of pathway activation was observed across patients and stimulation settings, particularly in the internal capsule pathways and the ansa lenticularis. Interhemispheric asymmetry could be caused by asymmetric lead locations, asymmetric stimulation settings, asymmetric electrode impedances, or a combination of these factors. Our data show that relatively few stimulation

Table 3. Correlations of Pathway Activation and Obsessive-Compulsive Behavior Improvement

Pathway	Correlation Coefficient (r_p)	95% CI	p Value
Associative Pallido-subthalamic	.34	.34–.35	.007[a]
Sensorimotor Pallido-subthalamic	.42	.41–.43	<.001[a]
Lenticular Fasciculus	.20	.20–.21	.139
Ansa Lenticularis	.03	.02–.04	.801
IC: Prefrontal Cortex	.53	.53–.54	<.001[a]
IC: Premotor Cortex	.44	.43–.44	<.001[a]
IC: Motor Cortex	.40	.39–.40	.002[a]

CI, confidence interval; IC, internal capsule; r_p, Pearson correlation.
[a]$p < .05$, false discovery rate corrected.

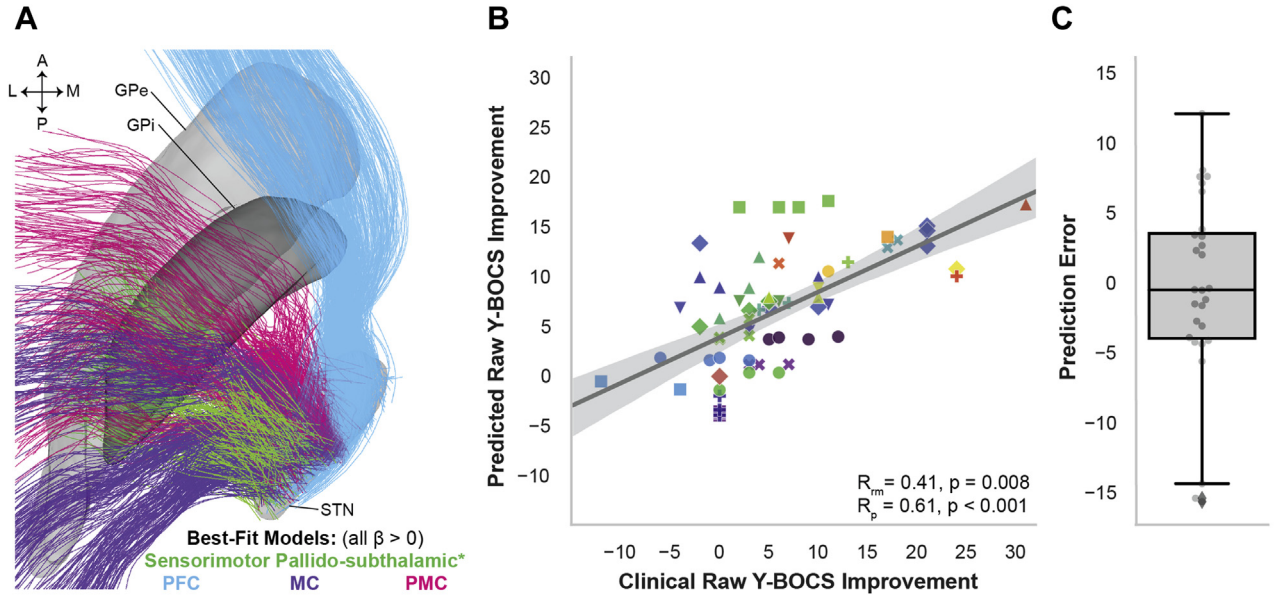

Figure 3. Obsessive-compulsive behavior improvement predicted using baseline severity and bilateral percent activation of the sensorimotor pallido-subthalamic pathway. **(A)** Visualization of the pathways identified in the best-fit models of obsessive-compulsive behavior improvement (models 1–4 in Table S3). **(B)** The best-fit model with the minimum Akaike information criterion (model 1 in Table S3) was predictive of raw Yale-Brown Obsessive Compulsive Scale (Y-BOCS) improvement scores for patients in the cohort ($n = 28$) across time points ($n = 68$). Individual patients are denoted by unique color-marker pairs. **(C)** Boxplot and individual data points of the prediction error in k-fold cross-validation, in which error = clinical score – predicted score. A, anterior; GPe, globus pallidus externus; GPi, globus pallidus internus; L, lateral; M, medial; MC, motor cortex; P, posterior; PFC, prefrontal cortex; PMC, premotor cortex; r_p, Pearson correlation; r_{rm}, repeated-measures correlation; STN, subthalamic nucleus.

settings were asymmetric across hemispheres, which suggests that stimulation settings were not commonly titrated on a per-hemisphere basis in the present cohort. The data also suggest that asymmetric lead locations likely contributed more to the asymmetry than different stimulation settings across hemispheres. Interhemispheric differences in lead locations may be intentional, due to anatomical asymmetry within a patient (42), or unintentional, due to stereotactic error (43) or to brain shift during lead implantation (44). Brain shift would be evident by a shift in lead location in the second implanted hemisphere, which was observed in our previous study (24), but it needs to be confirmed in future studies. Because this study was based on retrospective data, we were unable to compare the therapeutic effects of stimulation in one hemisphere over the other with sufficient statistical power. However, image-based predictors, including structural connectivity (26) and the fiber pathways in the present study, may enable DBS clinician programmers to refine stimulation settings within each hemisphere while accounting for lead location asymmetry. Future prospective studies should further investigate the contributions of stimulation in each individual hemisphere to the therapeutic response to DBS for TS.

Tic Improvement Involves the Associative Pallido-subthalamic Pathway

The results of this study indicate that GPi DBS may reduce tic severity by stimulating the associative pallido-subthalamic pathway, the ansa lenticularis, and the prefrontal internal capsule pathway (Table 2). However, the best-fit model indicates that improvement may be mainly mediated by stimulation of the associative pallido-subthalamic pathway (Table S2, Figure 2A). Importantly, the best-fit model predicted out-of-sample data through cross-validation, which suggests that this model could be applied to de novo patients.

The "associative" pallido-subthalamic pathway connects the anterior pallidum (within the globus pallidus externus and crossing through the GPi) and the anterior subthalamic nucleus, which includes both the associative and limbic subdivisions (45–47); therefore, the effects may be mediated by associative and/or limbic CBGTC networks. The involvement of associative and limbic networks in tic improvement following GPi DBS agrees with the results of our previous study showing that connectivity to the prefrontal cortex was associated with improvement (26). Additionally, neuroimaging research has shown that structural and functional changes in associative and limbic networks are linked to TS symptoms (48–51). Therefore, DBS likely improves symptoms through modulating activity in distributed pathological networks, and the associative pallido-subthalamic pathway may mediate the effects.

The involvement of the associative pallido-subthalamic pathway in tic improvement suggests that the anteromedial (limbic/associative) GPi may be more effective than the posteroventral (sensorimotor) GPi. However, previous studies have reported substantial tic improvement with DBS targeted to the posteroventral GPi (27,52,53). Based on the present results, the therapeutic effects of posteroventral GPi DBS may be due to modulation of posterior fibers in the associative pallido-subthalamic pathway, or modulation of the ansa lenticularis,

which courses from the posteroventral GPi and inferior to the anterior GPi. These two targets may also operate through different functional mechanisms; the posteroventral pallidum may directly suppress tic execution via sensorimotor networks (50,54), while the anteromedial GPi (i.e., the associative pallido-subthalamic pathway) may enhance the ability to suppress tics via associative and limbic networks (55–57). Additionally, the sensorimotor, associative, and limbic pathways may not be as distinctly segregated as previously thought (58,59), and these networks are functionally integrated to some degree (60,61). Thus, tic improvement with DBS likely involves a combination of CBGTC networks to improve the complex motor and behavioral symptoms of TS.

Based on our findings, the anterior associative/limbic subregions of the subthalamic nucleus may be a potential DBS target for TS. The anterior subthalamic nucleus has been reported to be an effective target for DBS for OCD (62,63), and studies in nonhuman primates have shown that high-frequency stimulation of the anterior subthalamic nucleus reduced stereotyped behaviors resembling those observed in TS and OCD (64). Additionally, preliminary studies have reported tic improvement with motor subthalamic nucleus DBS in patients with TS (23,65,66). The subthalamic nucleus may be advantageous for a heterogeneous disorder such as TS; it is smaller than the GPi and may allow for simultaneous modulation of associative, limbic, and sensorimotor networks with relatively low stimulation amplitudes, which could be titrated based on motor and behavioral symptoms.

OCB Improvement Involves the Sensorimotor Pallido-subthalamic Pathway and Internal Capsule

The results indicate that activation of the sensorimotor pallido-subthalamic pathway was particularly important in mediating OCB improvement, and the level of activation of this pathway combined with baseline severity significantly predicted outcomes across the cohort and for out-of-sample data. There was also substantial evidence to support the involvement of the internal capsule pathways projecting to the prefrontal cortex, motor cortex, and premotor cortex (Table S3, Figure 3A). Interestingly, these results indicate that OCB improvement may depend on modulating a combination of sensorimotor, associative, and limbic networks.

The involvement of the prefrontal and premotor internal capsule pathways in OCB improvement agrees with our previous study showing that associative/prefrontal and premotor networks are involved in improvement in OCB in patients receiving GPi DBS for TS (26). No other studies have investigated correlates of OCB reduction in patients with TS to the best of our knowledge. However, previous open-label studies have reported that transcranial magnetic stimulation to the supplementary motor area, part of the premotor network, reduces OCB in patients with TS (67–69). Additionally, the present results may be of interest for future studies of DBS for treatment-refractory OCD without TS. Previous studies have shown that the clinical efficacy of DBS for OCD was associated with modulation of associative and limbic networks, including prefrontal networks (35,70–72). In line with these studies, our results confirm the involvement of specific fiber pathways projecting to the prefrontal cortex that have been previously associated with OCD improvement across surgical targets for DBS for OCD, as reported by Li *et al.* (35). Therefore, activation of these prefrontal fiber pathways may improve OCD symptoms across primary diagnoses (i.e., OCD vs. TS with comorbid OCB). Additionally, our results suggest that anteromedial GPi DBS could be a viable surgical target to improve OCD symptoms by modulating these therapeutic fiber pathways. These results collectively support the idea that that modulation of pathways involved in prefrontal and premotor networks is associated with improvement in OCB in patients with or without TS; therefore, these networks could potentially be used to perform symptom-guided therapy.

In contrast, our results also indicate that OCB improvement in patients with TS is associated with modulation of the sensorimotor pallido-subthalamic pathway and of the internal capsule projecting to the motor cortex. Although surprising, this finding may indicate that the mechanisms are specific to the pathophysiology of comorbid OCB in TS, which has been hypothesized to differ from OCD alone (73,74). Studies have found that patients with TS and comorbid OCB experience less anxiety or cognitive phenomena and more sensory phenomena preceding repetitive behaviors than patients with OCD without TS (75,76), which may partially explain the involvement of sensorimotor networks. Previous neuroimaging studies have reported that TS with comorbid OCB is associated with structural, functional, and metabolic changes in limbic and associative areas, similar to patterns found across OCD cohorts (77). However, in patients with TS and comorbid OCB, these changes also extend into the motor cortex and supplementary motor area (49,78,79). Therefore, our results suggest that improvement in comorbid OCB in TS DBS patients may involve modulating the prefrontal, sensorimotor, and premotor pathways, which differs from what is known about DBS for OCD. Additional studies are needed to investigate the underlying mechanisms as they relate to the specific pathophysiology of TS and comorbid OCB.

The Role of Stimulation Duration in Symptom Improvement

Stimulation duration alone may not be a key factor in predicting symptom improvement, as the models with only follow-up time point and baseline severity had essentially no empirical support compared with the best-fit pathway activation models (Tables S2 and S3). Our previous research showed that there may be a long time course, on the order of months, for tic improvement with DBS (24), and other studies report similar time courses of the response to DBS for OCD (80,81) and dystonia (82,83). It remains unclear whether it requires months for symptoms to respond to DBS or to identify effective stimulation parameters. The present results indicate that tic and OCB improvement are more dependent on stimulation parameters and activation of specific pathways than just stimulation duration. Our findings suggest that the fiber pathways that were associated with tic or OCB improvement could be used to prospectively identify stimulation parameters for each hemisphere based on lead locations in individual patients. Applying such an optimization framework could potentially decrease the amount of time required to identify therapeutic settings and provide symptom relief to patients more quickly.

Implications for Targeting and Stimulation Programming

Our study found that modulation of specific basal ganglia and internal capsule pathways during GPi DBS for TS is linked to improvement in tics and comorbid OCB, and that activation of these pathways quantified by computational models of DBS could be used to predict outcome scores in future patients. These findings have important implications for both targeting and stimulation programming to reduce symptom severity effectively. A combination of lead location and stimulation settings is important for modulating the therapeutic pathways, and intuitively, a well-placed lead would require lower stimulation amplitudes to produce therapeutic effects. Indeed, based on the present findings and our previous work (26), lead location seems to be more imperative than stimulation settings in GPi DBS. Because the GPi is an elongated shape, a lead located in the far posterior subregion of the GPi would require relatively high stimulation amplitudes in order to reach the target pathways in the anterior GPi for tic improvement. Therefore, implanting in the anterior GPi would enable activating the target pathways and networks associated with tic improvement while limiting power consumption or side effects. Additionally, directional leads could be leveraged to steer the stimulation if the lead is within a few millimeters from the target pathway, and implanting multiple leads surrounding the target may provide more robust activation and finer control over the stimulation field (84).

Different pathways and stimulation targets may be more effective for specific clinical phenotypes of TS. The results of the present study provide a basis to further differentiate the fiber pathways associated with the response to DBS in specific symptom profiles, including variations in motor tics, vocal tics, and comorbidities. Given the heterogeneous symptoms across patients and a lack of acute biomarkers of response to stimulation, there is a critical need for data-driven, patient-specific approaches to programming DBS for TS. This is especially important because our previous results suggest that symptom improvement with DBS can be slow, perhaps because multiple programming sessions are often necessary to identify effective stimulation parameters (24). We envision a future in which clinicians could utilize an individual patient's baseline symptom severities, anatomy, and lead location to efficiently optimize stimulation settings to maximize activation of the therapeutic pathways in each hemisphere to alleviate the patient's symptoms.

Limitations

The present dataset was retrospective, and the majority of information was gleaned from open-label studies from several clinic sites and therefore may be biased. With so few TS cases implanted worldwide, it is imperative to pool data from multiple sites to yield generalizable knowledge, as we have reported in the present and previous studies (24,26). We utilized the YGTSS total score as a total measure of TS severity, including tic severity and overall impairment, which may be imperfect in measuring symptom severity. However, the variability in clinical rating scale scores was partially accounted for by using repeated measures per patient. Although our results are preliminary in understanding the therapeutic mechanisms of GPi DBS for TS, prospective studies are needed for validation.

We used tracts that were defined by expert neuroanatomists, with guidance from detailed histological atlases and MRI data (85). Using these tracts provided a reasonable estimate of each pathway's trajectory relative to surrounding nuclei; however, manual identification of these pathways may introduce biases that could influence the results, including variations in start/end points and tract density of the pathways. In particular, the ansa lenticularis tracts in the dataset do not traverse to the posterior GPi, as shown in previous anatomical studies (86). Additionally, the fiber pathways do not account for patient-specific variability or any TS-specific alterations in these pathways. Although diffusion-weighted imaging could potentially be used to delineate these tracts in individual patients, tractography has its own biases, and it can be difficult to reliably delineate pathways with complex geometries and crossing and kissing fibers (87,88). Other pathways may be relevant to the response to DBS for TS beyond the set of predetermined pathways. In our computational models, a single impedance value was used because patient-specific impedance measurements were not available, which may over- or underestimate the fiber tract activation in some patients. Additionally, we modeled fiber tract activation; however, other neurophysiological effects of stimulation may be relevant to the therapeutic mechanisms that could be explored in future studies.

ACKNOWLEDGMENTS AND DISCLOSURES

This work was supported by National Science Foundation Graduate Research Fellowship Program Grant No. 1747505 (to KAJ), National Institutes of Health (NIH) P41 Center for Integrative Biomedical Computing Grant No. GM103545 (to KAJ and CRB), NIH National Institute of Nursing Research Grant No. NR014852 (GD, CRB, and MSO), the National Institute for Health Research University College London Hospitals Biomedical Research Centre (to LZ, EMJ, and TF), an International TS Registry Grant from the Tourette Association of America (principal investigator: MSO), and NIH Grant No. R01NS096008 (to MSO).

This study was conducted in collaboration with the Tourette Syndrome Deep Brain Stimulation Working Group; for an updated list of contributing members, please visit the International Tourette Deep Brain Stimulation Database and Registry website (https://tourettedeepbrainstimulationregistry.ese.ufhealth.org/).

KAJ, GD, MH, EMJ, HA, DS, TFG, AB, MP, F-GM, AG, and WH report no biomedical financial interests or potential conflicts of interest. TF has received honoraria for speaking at meetings sponsored by Bill, Profile Pharma, and Boston Scientific; and received grant support from the National Institute of Health Research, Cure Parkinson's Trust, Michael J. Fox Foundation, Innovate UK, John Black Charitable Foundation, Van Andel Research Institute, and Defeat MSA. LZ acts as a consultant for Medtronic, Boston Scientific, and Elekta. AFGL has received a research grant from the Michael J. Fox Foundation and royalties from Springer media. KDF has received occasional consulting fees from Medtronic and Boston Scientific for deep brain stimulation (DBS)–related work. His research is funded by the National Institutes of Health and multiple foundation sources. Implantable devices for KDF's DBS-related research have been provided by Medtronic and NeuroPace. KDF has participated as a site implanting surgeon in multicenter DBS-related research studies sponsored by Abbott/St. Jude, Boston Scientific, and Functional Neuromodulation. The University of Florida receives partial funding for KDF's functional neurosurgery fellowship from Medtronic. KDF holds 3 DBS-related patents for which he has received no royalties. KDF is an associate editor for the *Journal of Parkinson's Disease*. MSO has served as a consultant for the National Parkinson Foundation and has received research grants from National Institutes of Health, National

Parkinson Foundation, the Michael J. Fox Foundation, the Parkinson Alliance, Smallwood Foundation, the Bachmann-Strauss Foundation, the Tourette Syndrome Association, and the University of Florida Foundation. MSO has previously received honoraria, but in the past >60 months has received no support from industry. MSO has received royalties for publications with Demos, Manson, Amazon, Smashwords, Books4Patients, and Cambridge (movement disorders books). MSO is an associate editor for *New England Journal of Medicine Journal Watch Neurology*. MSO has participated in continuing medical education and educational activities on movement disorders (in the last 36 months) sponsored by PeerView, Prime, QuantiaMD, WebMD, Medicus, MedNet, Henry Stewart, and Vanderbilt University. The institution and not MSO receives grants from Medtronic, AbbVie, Allergan, and Advanced Neuromodulation Systems/St. Jude, and the principal investigator has no financial interest in these grants. MSO has participated as a site principal investigator and/or co-investigator for several NIH-, foundation-, and industry-sponsored trials over the years but has not received honoraria. CRB has served as a consultant for NeuroPace, Advanced Bionics, Boston Scientific, Intelect Medical, St. Jude Medical, and Functional Neuromodulation; and he holds intellectual property related to DBS.

ARTICLE INFORMATION

From the Scientific Computing and Imaging Institute (KAJ, GD, CRB) and Departments of Biomedical Engineering (KAJ, GD, CRB), Neurology (CRB), Neurosurgery (CRB), and Psychiatry (CRB), University of Utah, Salt Lake City, Utah; Functional Neurosurgery Unit (TF, MH, LZ, EMJ, HA), Department of Clinical and Movement Neurosciences, Queen Square Institute of Neurology, University College London, London, United Kingdom; Department of Clinical Neuroscience (MH), Umea University, Umea, Sweden; Neurosurgical Department (DS, TFG, AB) and Tourette's Syndrome and Movement Disorders Center (MP), IRCCS Istituto Ortopedico Galeazzi, Milan, Italy; Beijing Neurosurgical Institute, (F-GM) Capital Medical University, Beijing, China; Department of Psychiatry and Neuropsychology (AFGL), Maastricht University Medical Centre, Maastricht, the Netherlands; Norman Fixel Institute for Neurological Diseases (AG, WH, KDF, MSO), Program for Movement Disorders and Neurorestoration, Departments of Neurology and Neurosurgery, University of Florida; and the J. Crayton Pruitt Family Department of Biomedical Engineering (AG), University of Florida, Gainesville, Florida.

Address correspondence to Christopher R. Butson, Ph.D., at butson@sci.utah.edu.

Received Aug 25, 2020; revised Oct 28, 2020; accepted Nov 14, 2020.

Supplementary material cited in this article is available online at https://doi.org/10.1016/j.bpsc.2020.11.005.

REFERENCES

1. Albin RL, Mink JW (2006): Recent advances in Tourette syndrome research. Trends Neurosci 29:175–182.
2. Albin RL (2018): Tourette syndrome: A disorder of the social decision-making network. Brain 141:332–347.
3. Hirschtritt ME, Lee PC, Pauls DL, Dion Y, Grados MA, Illmann C, *et al.* (2015): Lifetime prevalence, age of risk, and genetic relationships of comorbid psychiatric disorders in tourette syndrome. JAMA Psychiatry 72:325–333.
4. Kious BM, Jimenez-Shahed J, Shprecher DR (2016): Treatment-refractory Tourette syndrome. Prog Neuropsychopharmacology Biol Psychiatry 70:227–236.
5. Vandewalle V, van der Linden C, Groenewegen HJ, Caemaert J, Van Der Linden C, Groenewegen HJ, Caemaert J (1999): Stereotactic treatment of Gilles de la Tourette syndrome by high frequency stimulation of thalamus. Lancet 353:724.
6. Huys D, Bartsch C, Koester P, Lenartz D, Maarouf M, Daumann J, *et al.* (2016): Motor improvement and emotional stabilization in patients with Tourette syndrome after deep brain stimulation of the ventral anterior and ventrolateral motor part of the thalamus. Biol Psychiatry 79:392–401.
7. Welter M-L, Houeto J-L, Worbe Y, Diallo MH, Hartmann A, Tezenas du Montcel S, *et al.* (2019): Long-term effects of anterior pallidal deep brain stimulation for tourette's syndrome. Mov Disord 34:586–588.
8. Martinez-Ramirez D, Jiminez-Shahed J, Leckman JF, Porta M, Servello D, Meng F-G, *et al.* (2018): Efficacy and safety of deep brain stimulation in Tourette syndrome: The International Tourette Syndrome Deep Brain Stimulation Public Database and Registry. JAMA Neurol 75:353–359.
9. Kefalopoulou Z, Zrinzo L, Jahanshahi M, Candelario J, Milabo C, Beigi M, *et al.* (2015): Bilateral globus pallidus stimulation for severe Tourette's syndrome: A double-blind, randomised crossover trial. Lancet Neurol 14:595–605.
10. Ackermans L, Duits A, van der Linden C, Tijssen M, Schruers K, Temel Y, *et al.* (2011): Double-blind clinical trial of thalamic stimulation in patients with Tourette syndrome. Brain 134:832–844.
11. Maciunas RJ, Maddux BN, Riley DE, Whitney CM, Schoenberg MR, Ogrocki PJ, *et al.* (2007): Prospective randomized double-blind trial of bilateral thalamic deep brain stimulation in adults with Tourette syndrome. J Neurosurg 107:1004–1014.
12. Welter M-L, Houeto J-L, Thobois S, Bataille B, Guenot M, Worbe Y, *et al.* (2017): Anterior pallidal deep brain stimulation for Tourette's syndrome: A randomised, double-blind, controlled trial. Lancet Neurol 16:610–619.
13. Baldermann JC, Schüller T, Huys D, Becker I, Timmermann L, Jessen F, *et al.* (2016): Deep brain stimulation for Tourette-syndrome: A systematic review and meta-analysis. Brain Stimul 9:296–304.
14. Parent A, Hazrati L-N (1995): Functional anatomy of the basal ganglia. I. The cortico-basal ganglia-thalamo-cortical loop. Brain Res Rev 20:91–127.
15. Alexander GE, Crutcher MD (1990): Functional architecture of basal ganglia circuits: Neural substrates of parallel processing. Trends Neurosci 13:266–271.
16. Nair G, Evans A, Bear RE, Velakoulis D, Bittar RG (2014): The anteromedial GPi as a new target for deep brain stimulation in obsessive compulsive disorder. J Clin Neurosci 21:815–821.
17. Servello D, Galbiati TF, Balestrino R, Iess G, Zekaj E, Michele S De, Porta M (2020): Deep brain stimulation for Gilles de la Tourette syndrome: Toward limbic targets. Brain Sci 10:301.
18. Azriel A, Farrand S, Di Biase M, Zalesky A, Lui E, Desmond P, *et al.* (2020): Tractography-guided deep brain stimulation of the anteromedial globus pallidus internus for refractory obsessive-compulsive disorder: Case report. Neurosurgery 86:E558–E563.
19. Ji G-J, Liao W, Yu Y, Miao H-H, Feng Y-X, Wang K, *et al.* (2016): Globus pallidus interna in Tourette syndrome: Decreased local activity and disrupted functional connectivtiy. Front Neuroanat 10:93.
20. Jimenez-Shahed J, Telkes I, Viswanathan A, Ince NF (2016): GPi oscillatory activity differentiates tics from the resting state, voluntary movements, and the unmedicated Parkinsonian state. Front Neurosci 10:436.
21. Neumann W-J, Huebl J, Brücke C, Lofredi R, Horn A, Saryyeva A, *et al.* (2018): Pallidal and thalamic neural oscillatory patterns in Tourette syndrome. Ann Neurol 84:505–514.
22. Haense C, Müller-Vahl KR, Wilke F, Schrader C, Capelle HH, Geworski L, *et al.* (2016): Effect of deep brain stimulation on regional cerebral blood flow in patients with medically refractory tourette syndrome. Front Psychiatry 7:118.
23. Zhu G, Geng X, Zhang R, Chen Y, Liu Y, Wang S, Zhang J (2019): Deep brain stimulation modulates pallidal and subthalamic neural oscillations in Tourette's syndrome. Brain Behav 9:e01450.
24. Johnson KA, Fletcher PT, Servello D, Bona A, Porta M, Ostrem JL, *et al.* (2019): Image-based analysis and long-term clinical outcomes of deep brain stimulation for Tourette syndrome: A multisite study. J Neurol Neurosurg Psychiatry 90:1078–1090.
25. Akbarian-Tefaghi L, Akram H, Johansson J, Zrinzo L, Kefalopoulou Z, Limousin P, *et al.* (2017): Refining the deep brain stimulation target within the limbic globus pallidus internus for Tourette syndrome. Stereotact Funct Neurosurg 95:251–258.
26. Johnson KA, Duffley G, Anderson DN, Ostrem JL, Welter M, Baldermann JC, *et al.* (2020): Structural connectivity predicts clinical outcomes of deep brain stimulation for Tourette syndrome. Brain 143:2607–2623.
27. Zhang J-G, Ge Y, Stead M, Zhang K, Yan S, Hu W, Meng F-G (2014): Long-term outcome of globus pallidus internus deep brain stimulation in patients with Tourette syndrome. Mayo Clin Proc 89:1506–1514.

28. Deeb W, Rossi PJ, Porta M, Visser-Vandewalle V, Servello D, Silburn P, *et al.* (2016): The international deep brain stimulation registry and database for Gilles de la Tourette syndrome: How does it work? Front Neurosci 10:170.
29. Leckman JF, Riddle MA, Hardin MT, Ort SI, Swartz KL, Stevenson J, Cohen DJ (1989): The Yale Global Tic Severity Scale: Initial testing of a clinician-rated scale of tic severity. J Am Acad Child Adolesc Psychiatry 28:566–573.
30. Goodman WK, Price LH, Rasmussen SA, Mazure C, Fleischmann RL, Hill CL, *et al.* (1989): The Yale-Brown Obsessive Compulsive Scale. Arch Gen Psychiatry 46:1006–1011.
31. Avants BB, Epstein CL, Grossman M, Gee JC (2008): Symmetric diffeomorphic image registration with cross-correlation: Evaluating automated labeling of elderly and neurodegenerative brain. Med Image Anal 12:26–41.
32. Fonov V, Evans AC, Botteron K, Almli CR, McKinstry RC, Collins DL (2011): Unbiased average age-appropriate atlases for pediatric studies. Neuroimage 54:313–327.
33. Fonov V, Evans AC, McKinstry RC, Almli CR, Collins DL (2009): Unbiased nonlinear average age-appropriate brain templates from birth to adulthood. Neuroimage 47:S102.
34. Petersen MV, Mlakar J, Haber SN, Parent M, Smith Y, Strick PL, *et al.* (2019): Holographic reconstruction of axonal pathways in the human brain. Neuron 104:1056–1064.e3.
35. Li N, Baldermann JC, Kibleur A, Treu S, Akram H, Elias GJB, *et al.* (2020): A unified connectomic target for deep brain stimulation in obsessive-compulsive disorder. Nat Commun 11:3364.
36. Benjamini Y, Hochberg Y (1995): Controlling the false discovery rate: A practical and powerful approach to multiple testing. J R Stat Soc 57:289–300.
37. Akaike H (1973): Information theory and an extension of the maximum likelihood principle. In: Petrov BN, Caski F, editors. Proceeding of the Second International Symposium on Information Theory. Budapest, Hungary: Akademiai Kaido, 267–281.
38. Burnham KP, Anderson DR, editors. (2004). Model Selection and Multimodel Inference: A Practical Information-Theoretic Approach. New York: Springer.
39. Cavanaugh JE (1997): Unifying the derivations for the Akaike and corrected Akaike information criteria. Stat Probab Lett 33:201–208.
40. Bakdash JZ, Marusich LR (2017): Repeated measures correlation. Front Psychol 8:456.
41. Anderson DN, Duffley G, Vorwerk J, Dorval AD, Butson CR (2019): Anodic stimulation misunderstood: Preferential activation of fiber orientations with anodic waveforms in deep brain stimulation. J Neural Eng 16:016026.
42. Hirabayashi H, Tengvar M, Hariz MI (2002): Stereotactic imaging of the pallidal target. Mov Disord 17:S130–S134.
43. Burchiel KJ, McCartney S, Lee A, Raslan AM (2013): Accuracy of deep brain stimulation electrode placement using intraoperative computed tomography without microelectrode recording. J Neurosurg 119:301–306.
44. Miyagi Y, Shima F, Sasaki T (2007): Brain shift: An error factor during implantation of deep brain stimulation electrodes. J Neurosurg 107:989–997.
45. Lambert C, Zrinzo L, Nagy Z, Lutti A, Hariz M, Foltynie T, *et al.* (2012): Confirmation of functional zones within the human subthalamic nucleus: Patterns of connectivity and sub-parcellation using diffusion weighted imaging. Neuroimage 60:83–94.
46. Temel Y, Blokland A, Steinbusch HWM, Visser-Vandewalle V (2005): The functional role of the subthalamic nucleus in cognitive and limbic circuits. Prog Neurobiol 76:393–413.
47. Parent A, Hazrati LN (1995): Functional anatomy of the basal ganglia. II. The place of subthalamic nucleus and external pallidium in basal ganglia circuitry. Brain Res Rev 20:128–154.
48. Müller-Vahl KR, Grosskreutz J, Prell T, Kaufmann J, Bodammer N, Peschel T (2014): Tics are caused by alterations in prefrontal areas, thalamus and putamen, while changes in the cingulate gyrus reflect secondary compensatory mechanisms. B*MC Neurosci* 15:6.
49. Worbe Y, Gerardin E, Hartmann A, Valabrégue R, Chupin M, Tremblay L, *et al.* (2010): Distinct structural changes underpin clinical phenotypes in patients with Gilles de la Tourette syndrome. Brain 133:3649–3660.
50. Bohlhalter S, Goldfine A, Matteson S, Garraux G, Hanakawa T, Kansaku K, *et al.* (2006): Neural correlates of tic generation in Tourette syndrome: An event-related functional MRI study. Brain 129:2029–2037.
51. Nielsen AN, Gratton C, Church JA, Dosenbach NUF, Black KJ, Petersen SE, *et al.* (2019): Atypical functional connectivity in Tourette syndrome differs between children and adults. Biol Psychiatry 87:164–173.
52. Martínez-Fernández R, Zrinzo L, Aviles-Olmos I, Hariz M, Martinez-Torres I, Joyce E, *et al.* (2011): Deep brain stimulation for Gilles de la Tourette syndrome: A case series targeting subregions of the globus pallidus internus. Mov Disord 26:1922–1930.
53. Dehning S, Feddersen B, Cerovecki A, Botzel K, Muller N, Mehrkens JH (2011): Globus pallidus internus-deep brain stimulation in Tourette's syndrome: Can clinical symptoms predict response? Mov Disord 26:2440–2441.
54. Neuner I, Werner CJ, Arrubla J, Stocker T, Ehlen C, Wegener HP, *et al.* (2014): Imaging the where and when of tic generation and resting state networks in adult Tourette patients. Front Hum Neurosci 8:1–16.
55. Peterson BS, Skudlarski P, Anderson AW, Zhang H, Gatenby JC, Lacadie CM, *et al.* (1998): A functional magnetic resonance imaging study of tic suppression in Tourette syndrome. Arch Gen Psychiatry 55:326–333.
56. Kawohl W, Brühl A, Krowatschek G, Ketteler D, Herwig U (2009): Functional magnetic resonance imaging of tics and tic suppression in Gilles de la Tourette syndrome. World J Biol Psychiatry 10:567–570.
57. Ganos C, Kahl U, Brandt V, Schunke O, Baumer T, Thomalla G, *et al.* (2014): The neural correlates of tic inhibition in Gilles de la Tourette syndrome. Neuropsychologia 65:297–301.
58. Rossi PJ, Peden C, Castellanos O, Foote KD, Gunduz A, Okun MS (2017): The human subthalamic nucleus and globus pallidus internus differentially encode reward during action control. Hum Brain Mapp 38:1952–1964.
59. Parent A, Côté PY, Lavoie B (1995): Chemical anatomy of primate basal ganglia. Prog Neurobiol 46:131–197.
60. Haber SN (2003): The primate basal ganglia: Parallel and integrative networks. J Chem Neuroanat 26:317–330.
61. Joel D, Weiner I (1994): The organization of the basal ganglia-thalamocortical circuits: Open interconnected rather than closed segregated. Neuroscience 63:363–379.
62. Tyagi H, Apergis-Schoute AM, Akram H, Foltynie T, Limousin P, Drummond LM, *et al.* (2019): A randomized trial directly comparing ventral capsule and anteromedial subthalamic nucleus stimulation in obsessive-compulsive disorder: Clinical and imaging evidence for dissociable effects. Biol Psychiatry 85:726–734.
63. Mallet L, Polosan M, Jaafari N, Baup N, Welter M-L, Fontaine D, *et al.* (2008): Subthalamic nucleus stimulation in severe obsessive–compulsive disorder. N Engl J Med 359:2121–2134.
64. Baup N, Grabli D, Karachi C, Mounayar S, Francois C, Yelnik J, *et al.* (2008): High-frequency stimulation of the anterior subthalamic nucleus reduces stereotyped behaviors in primates. J Neurosci 28:8785–8788.
65. Vissani M, Cordella R, Micera S, Eleopra R, Romito L, Mazzoni A (2019): Spatio-temporal structure of single neuron subthalamic activity identifies DBS target for anesthetized Tourette Syndrome patients. J Neural Eng 16:066011.
66. Martinez-Torres I, Hariz MI, Zrinzo L, Foltynie T, Limousin P (2009): Improvement of tics after subthalamic nucleus deep brain stimulation. Neurology 72:1787–1790.
67. Mantovani A, Lisanby SH, Pieraccini F, Ulivelli M, Castrogiovanni P, Rossi S (2005): Repetitive transcranial magnetic stimulation (rTMS) in the treatment of obsessive–compulsive disorder (OCD) and Tourette's syndrome (TS). Int J Neuropsychopharmacol 9:95–100.
68. Chae J-H, Nahas Z, Wassermann E, Li X, Sethuraman G, Gilbert D, *et al.* (2004): A pilot safety study of repetitive transcranial magnetic

stimulation (rTMS) in Tourette's syndrome. Cogn Behav Neurol 17:109–117.
69. Mantovani A, Leckman JF, Grantz H, King R a, Sporn AL, Lisanby SH (2007): Repetitive transcranial magnetic stimulation of the supplementary motor area in the treatment of Tourette syndrome: Report of two cases. Clin Neurophysiol 118:2314–2315.
70. Baldermann JC, Melzer C, Zapf A, Kohl S, Timmermann L, Tittgemeyer M, *et al.* (2019): Connectivity profile predictive of effective deep brain stimulation in obsessive-compulsive disorder. Biol Psychiatry 85:735–743.
71. Hartmann CJ, Lujan JL, Chaturvedi A, Goodman WK, Okun MS, McIntyre CC, Haq IU (2016): Tractography activation patterns in dorsolateral prefrontal cortex suggest better clinical responses in OCD DBS. Front Neurosci 9:519.
72. Figee M, Luigjes J, Smolders R, Valencia-Alfonso CE, Van Wingen G, De Kwaasteniet B, *et al.* (2013): Deep brain stimulation restores frontostriatal network activity in obsessive-compulsive disorder. Nat Neurosci 16:386–387.
73. Anholt GE, Cath DC, Emmelkamp PMG, van Oppen P, Smit JH, van Balkom AJLM (2006): Do obsessional beliefs discriminate OCD without tic patients from OCD with tic and Tourette's syndrome patients? Behav Res Ther 44:1537–1543.
74. Jaisoorya TS, Reddy YCJ, Srinath S, Thennarasu K (2008): Obsessive-compulsive disorder with and without tic disorder: A comparative study from India. CNS Spectr 13:705–711.
75. Miguel EC, Baer L, Coffey BJ, Rauch SL, Savage CR, O'Sullivan RL, *et al.* (1997): Phenomenological differences appearing with repetitive behaviours in obsessive-compulsive disorder and Gilles de la Tourette's syndrome. Br J Psychiatry 170:140–145.
76. Cath DC, Spinhoven P, Hoogduin CAL, Landman AD, Van Woerkom TCAM, Van de Wetering BJM, *et al.* (2001): Repetitive behaviors in Tourette's syndrome and OCD with and without tics: What are the differences? Psychiatry Res 101:171–185.
77. Menzies L, Chamberlain SR, Laird AR, Thelen SM, Sahakian BJ, Bullmore ET (2008): Integrating evidence from neuroimaging and neuropsychological studies of obsessive-compulsive disorder: The orbitofronto-striatal model revisited. Neurosci Biobehav Rev 32:525–549.
78. Pourfar M, Feigin A, Tang CC, Carbon-Correll M, Bussa M, Budman C, *et al.* (2011): Abnormal metabolic brain networks in Tourette syndrome. Neurology 76:944–952.
79. Bhikram T, Arnold P, Crawley A, Abi-Jaoude E, Sandor P (2020): The functional connectivity profile of tics and obsessive-compulsive symptoms in Tourette syndrome. J Psychiatr Res 123:128–135.
80. Greenberg BD, Malone DA, Friehs GM, Rezai AR, Kubu CS, Malloy PF, *et al.* (2006): Three-year outcomes in deep brain stimulation for highly resistant obsessive-compulsive disorder. Neuropsychopharmacology 31:2384–2393.
81. Holland MT, Trapp NT, McCormick LM, Jareczek FJ, Zanaty M, Close LN, *et al.* (2020): Deep brain stimulation for obsessive–compulsive disorder: A long term naturalistic follow up study in a single institution. Front Psychiatry 11:55.
82. Krause M, Fogel W, Kloss M, Rasche D, Volkmann J, Tronnier V (2004): Pallidal stimulation for dystonia. Neurosurgery 55:1361–1368.
83. Ruge D, Tisch S, Hariz MI, Zrinzo L, Bhatia KP, Quinn NP, *et al.* (2011): Deep brain stimulation effects in dystonia: Time course of electrophysiological changes in early treatment. Mov Disord 26:1913–1921.
84. Janson AP, Anderson DN, Butson CR (2020): Activation robustness with directional leads and multi-lead configurations in deep brain stimulation. J Neural Eng 17:026012.
85. Petersen MV, Lund TE, Sunde N, Frandsen J, Rosendal F, Juul N, Østergaard K (2017): Probabilistic versus deterministic tractography for delineation of the cortico-subthalamic hyperdirect pathway in patients with Parkinson disease selected for deep brain stimulation. J Neurosurg 126:1657–1668.
86. Parent M, Parent A (2004): The pallidofugal motor fiber system in primates. Park Relat Disord 10:203–211.
87. Jones DK, Knösche TR, Turner R (2013): White matter integrity, fiber count, and other fallacies: The do's and don'ts of diffusion MRI. Neuroimage 73:239–254.
88. Thomas C, Ye FQ, Irfanoglu MO, Modi P, Saleem KS, Leopold DA, Pierpaoli C (2014): Anatomical accuracy of brain connections derived from diffusion MRI tractography is inherently limited. Proc Natl Acad Sci U S A 111:16574–16579.